# Dalton Transactions

An international journal of inorganic chemistry

www.rsc.org/dalton

Volume 42 | Number 11 | 21 March 2013 | Pages 3737–4092


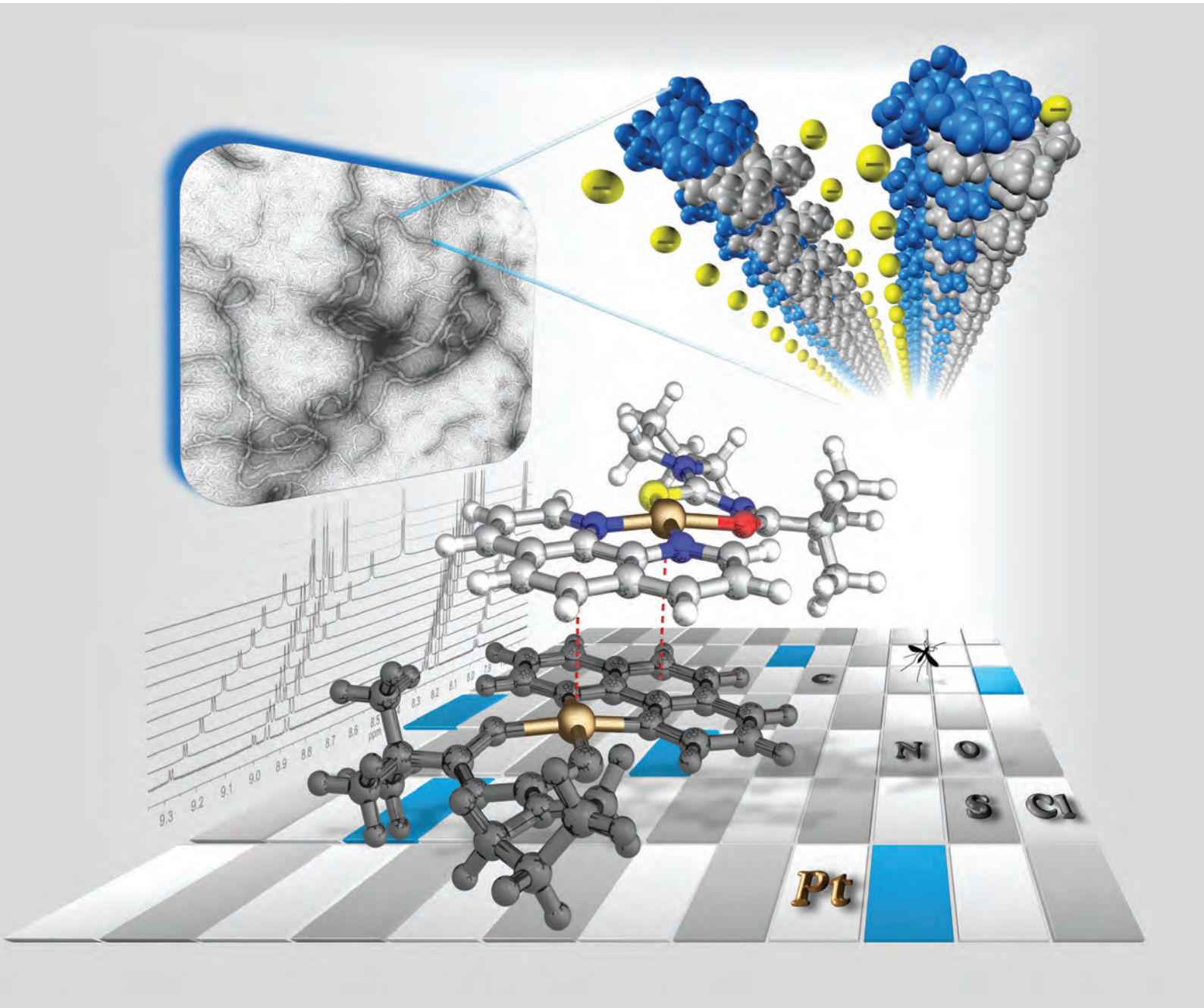



ISSN 1477-9226

RSC Publishing


**COVER ARTICLE**

Koch *et al.*

Cation–π induced aggregation of water-soluble $[Pt^{II}(diimine)(L^{n}\text{-}S,O)]^{+}$ complexes studied by $^{1}H$ DOSY NMR and TEM: from 'dimer aggregates' in acetonitrile to nano-aggregates ('metallogels') in water


1477-9226(2013)42:11;1-S

Dalton Transactions

RSC Publishing

PAPER

Cite this: *Dalton Trans.*, 2013, **42**, 3791

# Cation–π induced aggregation of water-soluble $[Pt^{II}(diimine)(L^n\text{-}S,O)]^+$ complexes studied by $^1H$ DOSY NMR and TEM: from 'dimer aggregates' in acetonitrile to nano-aggregates ('metallogels') in water†‡

Izak A. Kotzé, Wilhelmus J. Gerber, Yu-Shan Wu and Klaus R. Koch*

$^1H$ NMR chemical shift concentration dependence as well as the diffusion coefficients from DOSY NMR of mixed ligand $[Pt^{II}$(1,10-phenanthroline)(*N*-pyrrolidyl-*N*-(2,2-dimethylpropanoyl)thiourea)]Cl ($[Pt^{II}$-(phen)$(L^1\text{-}S,O)]$Cl) dissolved in mixtures of acetonitrile–water in the range 0–30% (v/v) $D_2O$–$CD_3CN$ shows that the complex cation ($M^+ = [Pt^{II}(phen)(L^1\text{-}S,O)]^+$) aggregates to form dimers, $2M^+ \rightleftharpoons \{M^+\}_2$, with association constants ranging from $K_D(CD_3CN) = 17 \pm 2\ M^{-1}$ to $K_D$(30% (v/v) $D_2O$–$CD_3CN) = $71 \pm 8\ M^{-1}$ at 299.3 K, presumably *via* non-covalent cation–π interactions. Experimental data are consistent with an 'offset' face-to-face cation–π stacking arrangement of the planar cation. However in water-rich solvent mixtures from >30% (v/v) $D_2O$–$CD_3CN$ to pure $D_2O$, the extent of aggregation significantly increases until a critical aggregation concentration (CAC) is reached, estimated to be 9.6 and 10.3 mM from $^1H$ NMR chemical shift concentration dependence and DOSY NMR measurements respectively. Above the CAC the formation of nano-structures formulated as $\{[Pt^{II}(phen)(L^1\text{-}S,O)]^+\}_n Cl^-_y$ ($n$, $y > 2$) is indicated. DOSY studies show a significant decrease of the average diffusion coefficient $D_{obs}$ as a function of increasing concentration of $[Pt^{II}(phen)(L^1\text{-}S,O)]$Cl in $D_2O$. The *aggregation number* ($N$) estimated from hydrodynamic volumes of the mononuclear $[Pt^{II}(phen)(L^1\text{-}S,O)]^+$ cation ($V_H^0$), and those $V_H$ estimated from $D_{obs}$ ($N = V_H/V_H^0$) as a function of total complex concentration, ranges from ~2 to ~735 in pure $D_2O$. Above the CAC well defined nano-structures which may be loosely termed "metallogels" could be characterized by means of transmission electron microscopy. As expected the addition of NaCl appears to increase the extent of aggregate formation, by presumably stabilizing the formation of nano-sized $\{[Pt^{II}$-(phen)$(L^1\text{-}S,O)]^+\}_n Cl^-_y$ aggregates preventing excessive positive electrostatic charge build-up.

Received 5th September 2012,
Accepted 14th November 2012

DOI: 10.1039/c2dt32053c

**www.rsc.org/dalton**

## Introduction

The 'self-association' of transition metal complexes, which display biological activity of potential pharmaceutical use, has been the subject of extensive interest in the last decade since their detailed physiochemical behaviour particularly in aqueous solution may have important implications on their mode of action.[1–5] Our interest in the chemistry of planar, cationic mixed-ligand $Pt^{II}$ complexes of the general type $[Pt^{II}$(diimine)$(L^n\text{-}S,O)]^+$ (where diimine is 2,2-bipyridine or 1,10-phenanthroline and $HL^n\text{-}S,O$ are various chelating *N*-acyl-*N*,*N*-dialkylthioureas) arises from their interesting biological activity ranging from potential anti-malarial activity[6] to DNA-intercalation and demonstrable *in vivo* activity toward bacterial *E. coli* AB1886 (uvr A) cultures.[7] Preliminary work also shows that such complexes undergo some interesting DNA-templated 'biomineralization'.[8] The *in vitro* anti-malarial activity[6] of $[Pt^{II}$-(diimine)$(L^n\text{-}S,O)]^+$ is postulated to arise from inhibition of β-hematin formation (synthetic hemozoin or malaria pigment) presumably as a result of the cationic planar complex $[Pt^{II}$-(diimine)$(L^n\text{-}S,O)]^+$ forming moderately strong outer-sphere aggregates with ferriprotoporphyrin IX, as can be demonstrated in 40% aqueous dimethyl sulfoxide (DMSO) solution, possibly through non-covalent cation–π interactions.[6] Moreover the $^1H$ NMR spectra of the series of cationic $[Pt^{II}$(diimine)-(*N*,*N*-di(*n*-butyl)-*N*′-benzoylthiourea]$^+$ complexes (as $PF_6^-$ salts where diimine = 1,10-phenanthroline, 4,7-diphenyl-1,10-phenanthroline, 2,2-bipyridyl, 4,4-di-*tert*-butyl-2,2-bipyridyl and

*Platinum Metals Chemistry Research Group, Department of Chemistry and Polymer Science, University of Stellenbosch, P Bag X1, Matieland, 7602, South Africa. E-mail: krk@sun.ac.za; Fax: ++2721 808 2344; Tel: ++2721 808 3020*

†This paper is dedicated to Professor Stefan Berger (Leipzig University), on the occasion of his retirement.

‡Electronic supplementary information (ESI) available: Consists of tables of all the $^1H$ and PFGE NMR data and related graphics. See DOI: 10.1039/c2dt32053c

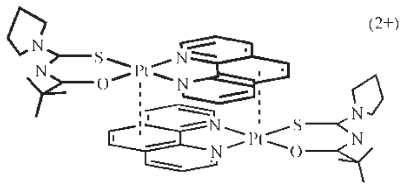

**Scheme 1** Postulated 'average' structure of a $\{[Pt^{II}(phen)(L^1\text{-}S,O)]^+\}_2$ dimer aggregate in solution based on $^1$H NMR shielding trends as a function of concentration.

4,4-dimethyl-2,2-bipyridyl) in acetonitrile at room temperature show significant concentration dependence, consistent with the formation of non-covalent dimer aggregates $2M^+ \rightleftharpoons \{M^+\}_2$ (where $M^+ = [Pt^{II}(diimine)(L^n\text{-}S,O)]^+$).[9] This concentration dependence of the $^1$H NMR chemical shifts can be used to estimate the association constants of such an aggregation process, while the relative spatial orientation of the molecules undergoing non-covalent association may be inferred from the extent of the relative changes in $^1$H NMR chemical shifts induced as a function of concentration.[9–12] A recent, detailed study of the water-soluble [Pt$^{II}$(1,10-phenanthroline)(*N*-pyrrolidyl-*N*-(2,2-dimethylpropanoyl)-thiourea)]Cl ([Pt$^{II}$(phen)(L$^1$-*S*,*O*)]-Cl) in acetonitrile showed that the non-covalent aggregation of the cationic $[Pt^{II}(phen)(L^1\text{-}S,O)]^+$ complexes results in dimer aggregates $2M^+ \rightleftharpoons \{M^+\}_2$ in solution (Scheme 1), while the $[Pt^{II}(phen)(L^1\text{-}S,O)]^+$ cation certainly forms non-covalent *hetero*-aggregates with aromatic molecules such as fluoranthene (F) corresponding to $M^+ + F \rightleftharpoons M^+F$ in acetonitrile, with an estimated association constant $K_B \sim 67 \pm 7$ M$^{-1}$ at room temperature.[13] Moreover, in water rich acetonitrile solutions the $^1$H NMR spectra of the $[Pt^{II}(phen)(L^1\text{-}S,O)]^+$ become progressively broader as the relative amount of water increases. This corresponds to similar unpublished observations of extremely broad, almost featureless $^1$H NMR spectra obtained in $D_2O$ at room temperature of the highly water-soluble complex [Pt$^{II}$(diimine)(*N*,*N*-di(2-hydroxyethyl)-*N*′-benzoylthiourea)]Cl (Fig. S1‡).[14] These interesting NMR spectra suggest formation of larger nano-scale aggregate structures in water of such cationic complexes,[14] the detailed nature of which has not been established to date.

We here report a study of the non-covalent aggregation behaviour of $[Pt^{II}(phen)(L^1\text{-}S,O)]^+$ cations in acetonitrile–water mixtures ranging from pure acetonitrile to pure water by means of the concentration dependence of the $^1$H NMR and Diffusion Ordered Spectroscopy (DOSY) techniques, supplemented by transmission electron microscopy to elucidate the nature of these phenomena, and the nano-aggregates which appear to form in water.

$^1$H diffusion ordered spectroscopy is a suitable technique for studying aggregation behaviour in solution since diffusion coefficients, which are very sensitive towards changes in the molecular/aggregate size, and the number of individual molecules, which constitute an aggregate, may be approximately estimated using the Stokes–Einstein equation.[15,16] Our aim is to mimic the biological media in which such complex cations may be active, particularly in the context of their potential anti-malarial activity *in vitro* and/or *in vivo*.[17]

## Results and discussion

### The effect of solvent composition (0–30% (v/v) $D_2O$–$CD_3CN$) on aggregation of [Pt$^{II}$(phen)(L$^1$-*S*,*O*)]Cl

In pure acetonitrile, the $^1$H NMR chemical shift concentration dependence trends (Fig. 1a) in 10% (v/v) $D_2O$–$CD_3CN$, as well as estimated diffusion coefficients by DOSY NMR (*vide infra*), of [Pt$^{II}$(phen)(L$^1$-*S*,*O*)]Cl can satisfactorily be accounted for by means of an aggregation model resulting in essentially exclusive formation of a $\{[Pt^{II}(diimine)(L^n\text{-}S,O)]^+\}_2$, consistent with a non-covalent cation–π association of $[Pt^{II}(phen)(L^1\text{-}S,O)]^+$ as demonstrated for related complexes previously.[9,13] However, by increasing the water content in these solutions, the $^1$H NMR resonances as a function of [Pt$^{II}$(phen)(L$^1$-*S*,*O*)]Cl concentration at 299.3 K become significantly broader as shown for 100% $D_2O$ in Fig. 1b. Moreover, all the $^1$H NMR peaks of the diimine moiety of the platinum complex show relatively larger upfield chemical shift displacements in the spectrum (peaks become more shielded) as the water content of the solutions increases, as well as on increasing concentration of the [Pt$^{II}$-(phen)(L$^1$-*S*,*O*)]$^+$ for a given acetonitrile–water mixture. Since only one set of resonance signals is observed in the $^1$H NMR spectra for the $[Pt^{II}(phen)(L^1\text{-}S,O)]^+$ complex/aggregate under any conditions, this is consistent with fast to intermediate exchange on the NMR timescale for the temperature range of 267.1 to 309.6 K. The relative upfield displacements of the $\delta_{obs}(H^2)$ and $\delta_{obs}(H^9)$§ resonances ($\delta$/ppm) of the diimine moiety of the $[Pt^{II}(phen)(L^1\text{-}S,O)]^+$ cation are significantly more pronounced compared to the $^1$H NMR signals of the *N*-acyl-*N*,*N*-dialkylthiourea moiety with increasing concentration (Fig. 1a) and increasing water content of the solvent mixture (Fig. 1b). The relative changes of $\delta_{obs}(H^{2/9})$/ppm induced as the concentration of [Pt$^{II}$(phen)(L$^1$-*S*,*O*)]Cl increases from 0.34 to 10.3 mM are significantly larger in pure $D_2O$ compared to acetonitrile ($\Delta^{max}\delta_{CD_3CN}$ = 0.28 ppm to $\Delta^{max}\delta_{D_2O}$ = 0.41 ppm). Similar trends have been reported for the related [Pt$^{II}$(diimine)-(*N*,*N*-di(*n*-butyl)-*N*′-benzoylthiourea)]$^+$ cation (Fig. S1‡).[14] The experimental trends of $\delta_{obs}(H^2)$ as a function of [Pt$^{II}$(phen)-(L$^1$-*S*,*O*)]Cl concentration in solutions up to 30% (v/v) $D_2O$–$CD_3CN$ at various temperatures are shown in Fig. 2. Non-linear least squares fitting of the experimental $\delta_{obs}(H^2)$ data to a dimer aggregate model $2M^+ \rightleftharpoons \{M^+\}_2$ ($M^+ = [Pt^{II}(phen)(L^1\text{-}S,O)]^+$) results in excellent agreement, allowing for estimated $K_D$ ($RSD_{max}$ < 13%) values in 0, 10, 20 and 30% (v/v) $D_2O$–$CD_3CN$ shown in Table 1 in a temperature range 282.6–309.6 K.

Standard reaction enthalpy ($\Delta_rH^0$) and entropy ($\Delta_rS^0$) values were estimated from the Van't Hoff plots shown in Fig. S2;‡ the good linear plots of Ln $K_D$ *vs.* $1/T$ are consistent with only a dimer $2M^+ \rightleftharpoons \{M^+\}_2$ equilibrium and rule out other possible

§ The protons H$^2$ and H$^9$ of the diimine moiety are most sensitive to changes in concentration and solvent composition.

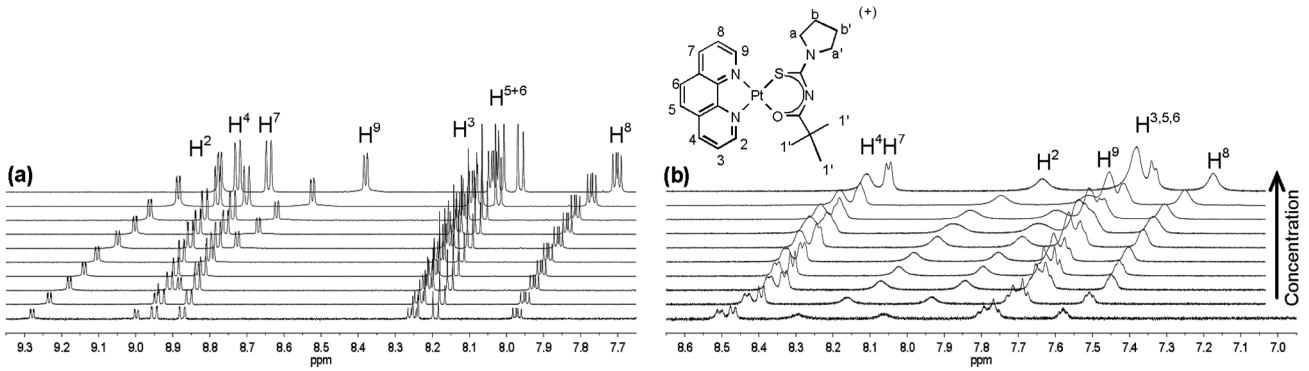


**Fig. 1** $^1$H NMR spectra (599.99 MHz) of $[Pt^{II}(phen)(L^1\text{-}S,O)]^+$ showing the chemical shift dependence of the 1,10-phenanthroline protons on the concentration of $[Pt^{II}(phen)(L^1\text{-}S,O)]^+$ in solutions containing (a) 10% (v/v) $D_2O$–$CD_3CN$ (0.3–26.4 mM, 299.3 K) and (b) $D_2O$ (0.3–25.0 mM, 309.6 K).

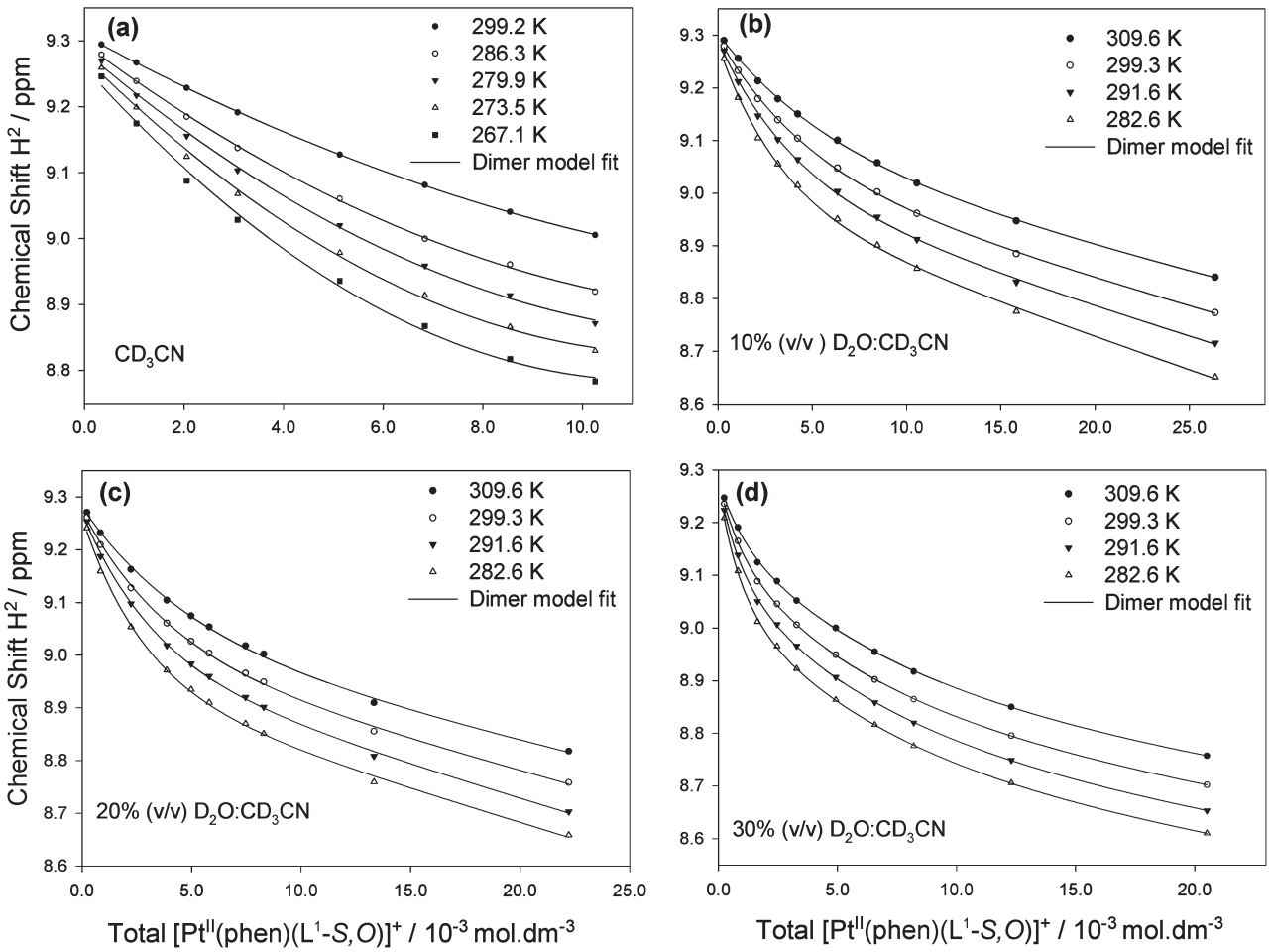


**Fig. 2** Excellent agreement between the dimer model least-squares fits and the experimental (symbols) chemical shift dependence of the 1,10-phenanthroline $H^2$ proton a concentration probe of $[Pt^{II}(phen)(L^1\text{-}S,O)]Cl$ in (a) 0 : 100, (b) 10 : 90, (c) 20 : 80 and (d) 30 : 70 (v/v) $D_2O$–$CD_3CN$ mixtures. (Calculated monomer and dimer chemical shifts available in the ESI Table S1.‡)

competing association processes or equilibria, such as ion-pairing and/or higher order aggregate formation for these solvent compositions (≤30% (v/v) $D_2O$–$CD_3CN$).

The increase in $K_D$ by a factor of 4–5 when the solvent composition is changed from pure acetonitrile to 30% (v/v) $D_2O$–$CD_3CN$ mixtures indicates that the dimer aggregate $\{[Pt^{II}(phen)(L^1\text{-}S,O)]^+\}_2$ is clearly favoured with increasing water ($D_2O$) content, as might be anticipated due to the expected hydrophobicity of such planar complex cations.

**Table 1** Thermodynamic data for the self-association of $[Pt^{II}(phen)(L^1\text{-}S,O)]^+$ in 0–30% (v/v) $D_2O$–$CD_3CN$ solutions as calculated from $^1H$ NMR chemical shift concentration and temperature dependence

| Percentage (v/v) $D_2O$–$CD_3CN$ | Temperature ($K$) | $K_D$ ($M^{-1}$) | $\Delta_rH^0$ (kJ mol$^{-1}$) | $\Delta_rS^0$ (J mol$^{-1}$ K$^{-1}$) | $\Delta_rG^0$ (kJ mol$^{-1}$) |
|---|---|---|---|---|---|
| 0 | 309.6 | 12 (±1) | | | |
| | 299.3 | 17 (±2) | −25.1 (±3.1) | −61 (±11) | −7.0 |
| | 291.6 | 22 (±2) | | | |
| | 282.6 | 29 (±3) | | | |
| 10 | 309.6 | 20 (±2) | | | |
| | 299.3 | 27 (±3) | −19.7 (±2.4) | −40 (±7) | −8.0 |
| | 291.6 | 33 (±3) | | | |
| | 282.6 | 41 (±5) | | | |
| 20 | 309.6 | 29 (±3) | | | |
| | 299.3 | 39 (±4) | −20.1 (±2.5) | −38 (±7) | −8.6 |
| | 291.6 | 43 (±4) | | | |
| | 282.6 | 64 (±7) | | | |
| | 309.6 | 54 (±5) | | | |
| 30 | 299.3 | 71 (±8) | −18.9 (±2.3) | −27 (±5) | −10.4 |
| | 291.6 | 87 (±9) | | | |
| | 282.6 | 109 (±10) | | | |

The process $2M^+ \rightleftharpoons \{M^+\}_2$ is evidently enthalpy driven ($\Delta_rH^0 < 0$) while a negative standard reaction entropy ($\Delta_rS^0 < 0$) is consistent with an aggregation/association process.[18] Interestingly the enthalpy of the dimer formation ($\Delta_rH^0$) decreases somewhat on passing from pure acetonitrile ($\Delta_rH^0 = -25.1$ kJ mol$^{-1}$) to a 10% (v/v) $D_2O$–$CD_3CN$ ($\Delta_rH^0 = -19.7$ kJ mol$^{-1}$) mixture, after which the reaction enthalpy remains essentially constant within experimental error for 20 and 30% (v/v) $D_2O$–$CD_3CN$ solutions. By contrast the $\Delta_rS^0$ becomes systematically less negative as the $D_2O$ content increases, Table 1. Doty and Myers attributed similar trends in $\Delta\Delta_rS^0$ for dimerization of protein moieties to the dehydration of charged groups upon aggregation, while Kauzmann and Scheraga suggested that this trend may be due to non-covalent hydrophobic bonding of non-polar groups increasing the degree of freedom of the water molecules close to hydrophobic groups.[19–21] It is thus reasonable to postulate that the trends in $\Delta\Delta_rS^0$ observed in this study may be attributed to the "hydrophobicity" of the coordinated 1,10-phenanthroline moiety, the effects of which become more significant as the solvent polarity increases with increasing water content of the solvent mixture (dielectric constant, $\varepsilon_{water} = 78.5$ and $\varepsilon_{acetonitrile} = 37.5$).[22,23]

The $\delta(^1H)$ trend differences for $^1H$ peaks of the 1,10-phenanthroline moiety as compared to butyl and *N*-pyrrolidyl $^1H$ signals of $[Pt^{II}(phen)(L^1\text{-}S,O)]^+$ as a function of concentration and temperature are entirely consistent with a *regiospecific* face-to-face stacking arrangement of the $[Pt^{II}(phen)(L^1\text{-}S,O)]^+$ cations in a dimer (Scheme 1) in these solutions up to 30% (v/v) $D_2O$–$CD_3CN$ as previously postulated in pure acetonitrile.[9,13] Essentially the two planar complex cations interact with one another through cation–π interactions in a characteristic 'offset' stacking configuration consistent with the model proposed by Hunter and Sanders[24] in their study on the nature of "π-stacking interactions" based on porphyrin–porphyrin aggregation.

The observed shielding trends as a function of concentration particularly of the $H^2$ and $H^9$ protons of the coordinated diimine moiety clearly rule out a possible "T-shaped" cation–π interaction in these solutions.[24]

### Aggregation behaviour of $[Pt^{II}(phen)(L^1\text{-}S,O)]Cl$ in water-rich mixtures >30% (v/v) $D_2O$–$CD_3CN$

In water-rich acetonitrile >30% (v/v) $D_2O$–$CD_3CN$ mixtures significantly broader $^1H$ NMR resonances are observed for all the $^1H$ peaks associated with the diimine moiety in $[Pt^{II}(phen)(L^1\text{-}S,O)]^+$ (Fig. 1b), eventually resulting in poorly resolved $^1H$ NMR spectra. Additionally, the even more pronounced shielding of the $H^2$ and $H^9$ protons of the diimine moiety with increasing $[Pt^{II}(phen)(L^1\text{-}S,O)]^+$ concentrations suggests the formation of a larger scale structure/aggregate in solution. Significantly, application of a simple dimer $2M^+ \rightleftharpoons \{M^+\}_2$ model to the experimentally observed $^1H$ NMR shielding trends fails to account for these satisfactorily, particularly as the water content of the solvent increases to pure $D_2O$.

The significant line-broadening of $^1H$ NMR peaks in $D_2O$ may be associated with a decrease in the $T_2$ relaxation times as estimated from $^1H$ NMR peak width at half-height ($\Delta\upsilon_{1/2} \propto 1/T_2$) under optimum magnetic field homogeneities.[25,26] The measured $^1H$ NMR resonance half-height ($\Delta\upsilon_{1/2}$) of the $H^{2/9}$ resonances in $[Pt^{II}(phen)(L^1\text{-}S,O)]^+$ increases from 0.9 Hz in pure $CD_3CN$ to 18 Hz in pure $D_2O$ at constant temperature. The extremely pronounced $^1H$ NMR broadening observed for $[Pt^{II}(diimine)(N,N\text{-di(2-hydroxyethyl)-}N'\text{-benzoylthiourea})]Cl$ (Fig. S1‡) in $D_2O$, and an inverse dependence of line-width with temperature[14] undoubtedly indicate that whatever the nature of the aggregate structure(s) formed in solution must have significantly larger average molecular weights.[27] We postulate that non-covalent *inter*-molecular interactions associated with the formation of large nano-sized aggregates with high molecular weight $D_2O$ are likely to result in significant shortening of the $T_2$ relaxation times consistent with larger structures and thus longer molecular correlation/tumbling times $\tau_c$ commonly associated with macromolecules.[26–28] The greater degree of shielding of *inter alia* $H^{2/9}$ with increasing complex

 

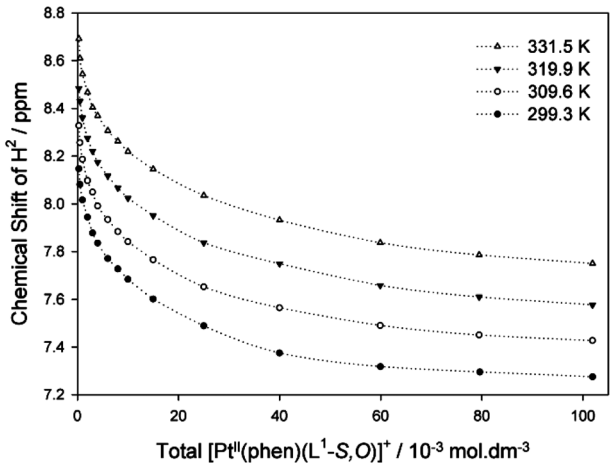


**Fig. 3** The $^1$H NMR chemical shift dependence of $H^2$ on [$Pt^{II}$(phen)($L^1$-*S*,*O*)]Cl concentration in $D_2O$ at temperatures 299.3, 309.6, 319.9, and 331.5 K. (Note: the dotted lines are aids for trend visualization.)

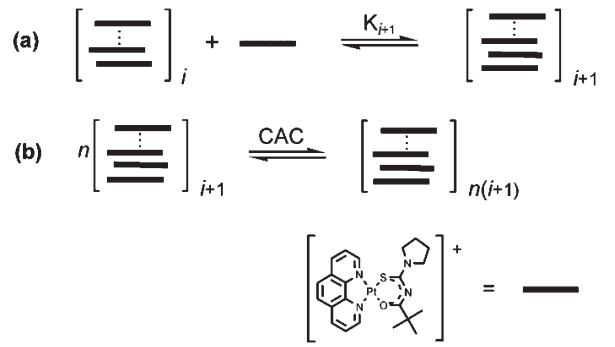


**Scheme 2** Postulated aggregation model of [$Pt^{II}$(phen)($L^1$-*S*,*O*)]Cl in aqueous solutions consisting of two major equilibrium processes with (a) an accumulative aggregation with $K_i$ the respective association constant corresponding to the *i*th monomer associating to the aggregate and (b) the formation of nano-sized aggregates after a specific critical aggregation concentration (CAC).

concentration in $D_2O$ (due to the chemical shift anisotropy (CSA) phenomenon) illustrated by the data in Fig. 3 for several temperatures is consistent with more extensive cation–π aromatic-ring stacking expected for the planar quasi-aromatic [$Pt^{II}$(phen)($L^1$-*S*,*O*)]$^+$ cation. Despite our best efforts, the shielding trends in $D_2O$ and (water rich solutions > (v/v) $D_2O$–$CD_3CN$) could also not be satisfactorily accounted for by simple or even higher order aggregation models such as trimer-, tetramer formation, *etc.* We therefore propose a multiple aggregate formation model leading to the formation of structures formulated as $\{[Pt^{II}(phen)(L^1\text{-}S,O)]^+\}_n Cl^-_y$ (*n* and *y* variable but >2) similar to a model proposed for procyanidin aggregation in a wine-like medium described by Pianet *et al.*,[29] illustrated in Scheme 2.

Our experimental NMR data in $D_2O$ are consistent with a model described in Scheme 2, in which at relatively low total complex concentrations initially, (a) the self-association of [$Pt^{II}$(phen)($L^1$-*S*,*O*)]$^+$ cations results in dimer aggregates, which however eventually lead to the formation of $\{[Pt^{II}(phen)(L^1\text{-}S,O)]^+\}_n Cl^-_y$ structures *via* an unspecified number of sequential equilibria ($K_{i+1}$), as the total complex concentration increases; (b) above a certain critical concentration of [$Pt^{II}$(phen)($L^1$-*S*,*O*)]$^+$, which may for convenience be termed a 'critical aggregation concentration' (CAC), similar to the well-known critical micelle concentration (CMC), larger nano-sized aggregate structures appear to form with concomitant ion-pair formation by $Cl^-$ ions, to offset excessive positive charge build-up as a result of the formation of a charged 'cation-aggregate' (Scheme 2b).[29]

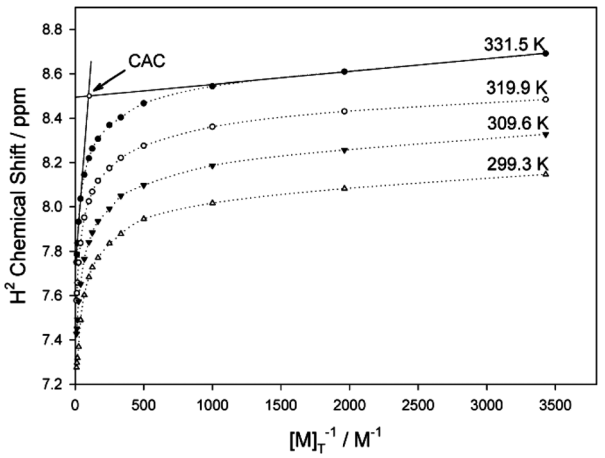


**Fig. 4** The observed $^1$H chemical shift of $H^2$ at temperatures 299.3–331.5 K against 1/$[M]_T$ were $[M]_T$ = Total [$Pt^{II}$(phen)($L^1$-*S*,*O*)]Cl concentration in $D_2O$. The expansions and extrapolations of the $^1$H NMR chemical shift concentration dependence of all temperatures are displayed in Fig. S3.‡ (Note: the dotted lines are aids for trend visualization.)

**Table 2** Estimated critical aggregation concentrations (CAC) in $D_2O$ from concentration dependence $\delta_{obs}(H^2)$ data at various temperatures, as well as diffusion coefficient ($D_{obs}$) dependence on concentration at 299.3 K

| Temp (K) | 299.3 | 309.6 | 319.9 | 331.5 |
|---|---|---|---|---|
| $\delta$, CAC mM | 9.6 (±0.6) | 12.0 (±0.7) | 13.9 (±0.9) | 14.9 (±0.9) |
| *D*, CAC mM | 10.3 (±1.5) | | | |

In support of such a CAC model, a plot of $\delta_{obs}(H^2)$ of [$Pt^{II}$(phen)($L^1$-*S*,*O*)]$^+$ against 1/$[M]_T$ ($[M]_T$ = total [$Pt^{II}$(phen)($L^1$-*S*,*O*)]Cl concentration) results in two quasi-linear regions (Fig. 4), the intercept of such lines gives an estimate of the critical aggregation concentration[30,31] in $D_2O$ for the [$Pt^{II}$(phen)($L^1$-*S*,*O*)]$^+$ complex as listed in Table 2. The estimated CAC for [$Pt^{II}$(phen)($L^1$-*S*,*O*)]$^+$ increases with temperature as may be expected given that the aggregation process is enthalpy driven ($\Delta_r H^0 < 0$), suggested by data in Table 1.

## Effect of chloride ion concentration on [$Pt^{II}$(phen)($L^1$-*S*,*O*)]$^+$ aggregation in water

The extent of aggregation of cationic [$Pt^{II}$(phen)($L^1$-*S*,*O*)]$^+$ complexes to form dimer $\{M\}_2^{2+}$ type structures in mainly acetonitrile and in water the postulated nano-scale aggregate structures $\{[Pt^{II}(phen)(L^1\text{-}S,O)]^+\}_n$ is likely to lead to

electrostatic positive charge build-up, which is probably partially offset by the chloride ion ion-paring/association in solution. Thus the effective $Cl^-$ : cation ratio may be expected to stabilize and/or affect the formation of aggregate structures in $D_2O$. This is confirmed by the significant shielding induced in the $\delta_{obs}(H^2)$ peak of the 1,10-moiety of $[Pt^{II}(phen)(L^1\text{-}S,O)]^+$ on "titration" of a 4.54 mM solution of $[Pt^{II}(phen)(L^1\text{-}S,O)]^+$ below the CAC, with NaCl solution in $D_2O$ increasing the effective $[Cl]^-$ from 10.5 to 346.7 mM, as illustrated in Fig, S4,‡ corresponding to a $Cl^-$ : cation ratio of *ca.* 2 to 77. Further increases to a $Cl^-$ : cation ratio to >80 lead to precipitation of a yellow solid from solution. The shielding induced in $\delta_{obs}(H^{2/9})$ as a result of increasing the $Cl^-$ : cation ratio cannot be solely due to ionic strength increases, since the corresponding $^1H$ NMR chemical shifts of the butyl and *N*-pyrrolidyl protons are comparatively small compared to the diimine protons, while the residual solvent peak and any minor impurities in the $^1H$ NMR spectrum remain essentially unaffected over the titration range. These trends suggest that the overall 'size' of the nano-scale aggregate $\{[Pt^{II}(phen)(L^1\text{-}S,O)]^+\}_n Cl^-_y$ appears to grow in size ($n$, $y$ increase) or at least be stabilized with increasing $Cl^-$ : cation ratio, until precipitation from solution occurs, akin to the well-known "salting-out" phenomenon.

Thus in water, or at least in water-rich acetonitrile mixtures above 30% (v/v) $D_2O$–$CD_3CN$, the proposed positively charged aggregate structures of the $[Pt^{II}(phen)(L^1\text{-}S,O)]^+$ complex cation as envisaged in Scheme 2 may be reasonably represented by eqn (1):

$$\{[Pt^{II}(\text{phen})(L^1-S,O)]^+\}_n Cl^-_y + x[Pt^{II}(\text{phen})(L^1-S,O)]^+ + zCl^- \rightleftharpoons \{[Pt^{II}(\text{phen})(L^1-S,O)]^+\}_{(n+x)} Cl^-_{(y+z)} \quad (1)$$

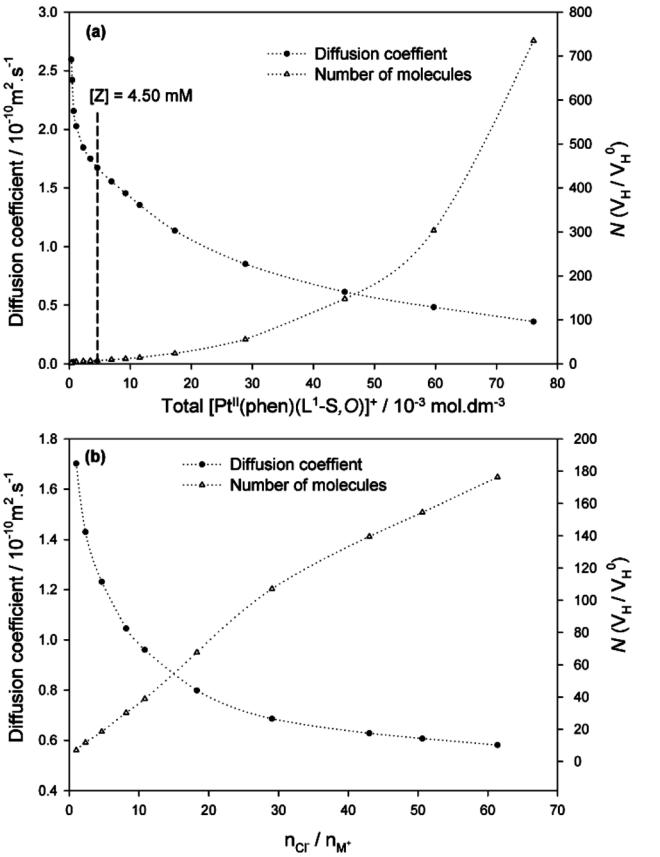


**Fig. 5** (a) $[Pt^{II}(phen)(L^1\text{-}S,O)]Cl$ diffusion coefficient ($D_{obs}$) and average aggregation number ($N$) ($N = V_H/V_H^0$) as a function of $[Pt^{II}(phen)(L^1\text{-}S,O)]Cl$ concentration in pure $D_2O$. (b) The effect of $Cl^-$ addition (NaCl) on the diffusion coefficient of $[Pt^{II}(phen)(L^1\text{-}S,O)]Cl$ (concentration indicated as [Z]) and the calculated average number of molecules ($N$) with $n_{Cl-}/n_{M+}$ the mole ratio of $Cl^-$ over $[Pt^{II}(phen)(L^1\text{-}S,O)]^+$ in $D_2O$.

## Diffusion ordered NMR spectroscopy

A semi-quantitative estimate of the effective number of complex cations ($n$) which may constitute the postulated nano-sized aggregate structure would lend convincing support to this model.

Based on the expectation that the translational diffusion of such aggregates in solution should depend significantly on their effective 'size' as suggested by the concentration dependence of $^1H$ NMR shielding data, $^1H$ DOSY NMR was used to study this phenomenon in solution. Data from DOSY NMR experiments in the concentration range 0.34–76.08 mM $[Pt^{II}(phen)(L^1\text{-}S,O)]^+$ at 299.3 K in $D_2O$ are shown in Fig. 5 and Table 3. Single exponential decay fits the attenuation of the $^1H$ DOSY NMR data very well, and indicates that the observed diffusion coefficient ($D_{obs}$) is an average of that of the mononuclear $[Pt^{II}(phen)(L^1\text{-}S,O)]^+$ and *all* aggregate species in solution ($D_{obs} = \alpha_m D_m + \ldots + \alpha_i D_i$) in solution. The $D_{obs}$ for the $[Pt^{II}(phen)(L^1\text{-}S,O)]^+$ in water shows a significant decrease as a function of concentration (Fig. 5a), consistent with a higher order aggregate formation.

**Table 3** Diffusion coefficient ($D$) concentration dependence data, calculated hydrodynamic radii ($r_H$) and average aggregation numbers ($N$), with $N = V_H/V_H^0$ where $V_H$ is the volume calculated from $r_H$ and $V_H^0$ the estimated volume of a monomer at infinite dilution

| Concentration ($10^{-3}$ mol dm$^{-3}$) | $D$ ($10^{-10}$ m$^2$ s$^{-1}$) | $r_H$ (Å) | $V_H$ (Å$^3$) | $N$ ($V_H/V_H^0$) |
|---|---|---|---|---|
| 76.08 | 0.36 | 56.1 | 739 692 | 735 |
| 59.72 | 0.52 | 39.1 | 250 561 | 304 |
| 45.14 | 0.61 | 32.9 | 148 577 | 148 |
| 28.84 | 0.85 | 23.7 | 55 532 | 55.2 |
| 17.31 | 1.14 | 17.7 | 23 345 | 23.2 |
| 11.54 | 1.35 | 14.9 | 13 818 | 13.7 |
| 9.230 | 1.47 | 13.7 | 10 708 | 11.1 |
| 6.922 | 1.55 | 13.0 | 9120 | 9.06 |
| 4.615 | 1.67 | 12.1 | 7335 | 7.29 |
| 3.462 | 1.77 | 11.4 | 6182 | 6.35 |
| 2.307 | 1.84 | 10.9 | 5458 | 5.42 |
| 1.154 | 2.05 | 9.84 | 3990 | 4.08 |
| 0.721 | 2.16 | 9.34 | 3415 | 3.39 |
| 0.481 | 2.42 | 8.32 | 2415 | 2.40 |
| 0.337 | 2.59 | 7.76 | 1961 | 1.95 |
| 0[a] | 3.24 | 6.22 | 1007 | 1 |

[a] Extrapolated to infinite dilution using the $D_{obs}$ *vs.* $1/[M]_T$ plot.

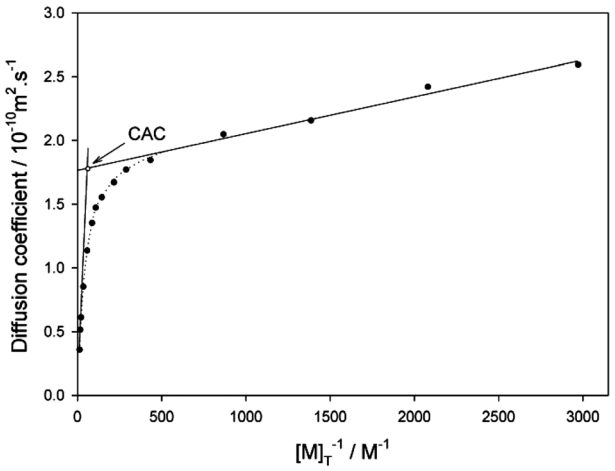


**Fig. 6** $[Pt^{II}(phen)(L^1\text{-}S,O)]^+$ diffusion coefficient at 299.3 K against $1/[M]_T$, were $[M]_T$ = Total $[Pt^{II}(phen)(L^1\text{-}S,O)]Cl$ concentration. (Note: The dotted lines are aids for trend visualization.)

The Stokes–Einstein equation $D = kT/6\pi\eta r_H$ may be used to estimate the hydrodynamic radii of species from the measured diffusion coefficients, where $k$ is the Boltzmann constant, $\eta$ the solvent viscosity, and $r_H$ the hydrodynamic radius. Since the diffusion coefficient obtained for $[Pt^{II}(phen)(L^1\text{-}S,O)]^+$ is the average between all species in solution, the $r_H$ is an average value. Although the Stokes–Einstein equation is only a crude approximation for estimating the 'size' of a square planar $[Pt^{II}(phen)(L^1\text{-}S,O)]^+$ complex, the changes in the average $r_H$ as a function of concentration may be useful to support the proposed aggregation model herein. The $r_H$ of a single monomer ($r_H^0$) has been estimated by extrapolating the $D_{obs}$ to infinite dilution from the plot of $D_{obs}$ *vs.* $1/[M]_T$, Fig. 6. An estimate of the CAC at *ca.* 10.3 ± 1.5 for this complex may also be obtained from this plot, which is in satisfactory agreement with the CAC values obtained by the simple $\delta(H^2)$ concentration dependence data shown in Table 2.

The extent of aggregation can be estimated by considering the *aggregation number* ($N$) calculated from the hydrodynamic volumes of the monomer ($V_H^0$) and $V_H$ estimated from $D_{obs}$ ($N = V_H/V_H^0$).[32] Table 3 lists the data obtained from this system from the $^1H$ DOSY NMR experiments at 299.3 K. The average aggregate-number in solution increases from $N \sim 1.95$ at the lowest practically measureable concentration by DOSY NMR of 0.34 mM of $[Pt^{II}(phen)(L^1\text{-}S,O)]^+$ with an estimated hydrodynamic radius of *ca.* 7.8 Å and $V_H$ = 1961 Å$^3$, to a maximum $N \sim$ 735 ($[M]_T$ = 76.1 mM) corresponding to a 'size' of *ca.* 735 nm$^3$ for the postulated nano-aggregate structure of $\{[Pt^{II}(phen)(L^1\text{-}S,O)]^+\}_nCl^-_y$ structure(s) in solution.

Significant changes in $D_{obs}$ are seen in $D_2O$ for a 4.5 mM $[Pt^{II}(phen)(L^1\text{-}S,O)]^+$ solution ([Z] dashed line in Fig. 5a) upon increasing the $Cl^-$ : cation ratio by means of 'titration' with NaCl. The 4.5 mM concentration was chosen well below the CAC value of 9.6 mM to show the maximum effect. In this way the calculated average aggregation number ($N$) of $[Pt^{II}(phen)(L^1\text{-}S,O)]^+$ increased from 8 to a maximum of *ca.* 176 for the highest practical $Cl^-$ : cation ratio ($n_{Cl-}/n_{M+}$), before precipitation occurs (Fig. 5b). The increase in NaCl concentration up to a maximum of ~342 mM might be expected to increase the viscosity of the solution significantly, although the estimated overall change in viscosity is at most *ca.* 0.02 mPa s$^{-1}$, which results in a difference of only *ca.* 1.8–2% in the calculated diffusion coefficients.[33] These data satisfactorily confirm the effect of increasing the $Cl^-$ : cation ratio on the postulated nano-aggregate ("metallogel") formation of $\{[Pt^{II}(phen)(L^1\text{-}S,O)]^+\}_nCl^-_y$ type structures in water, as summarized by the equilibrium (1) above. Such nano-aggregate structures are likely to be well within a size range possibly observable by means of transmission electron microscopy (TEM).

### Transmission electron microscopy (TEM)

TEM images obtained from 10–15 mM $[Pt^{II}(phen)(L^1\text{-}S,O)]Cl$ solutions in water and stained with uranyl acetate revealed the presence of well-defined 'spaghetti-like' aggregate structures with a diameter of *ca.* 20 nm, as shown in Fig. 7a. Similar TEM images have been obtained for the series of related highly water-soluble complexes $[Pt^{II}(diimine)(N,N\text{-di(2-hydroxyethyl)-}N'\text{-benzoyl-thiourea)}]Cl$ from unpublished studies,[14] of which a representative image is shown in ESI (Fig. S5‡). The maximum diameter of the spaghetti-like aggregates observed in the TEM images of $[Pt^{II}(phen)(L^1\text{-}S,O)]Cl$ appears to be limited to *ca.* 20 nm, with the uranyl acetate stain accumulating at the surface/edges of these aggregates. Images obtained from $[Pt^{II}(phen)(L^1\text{-}S,O)]Cl$ from pure acetonitrile solutions confirm that the extent of aggregation from acetonitrile solutions is significantly less pronounced, resulting in only poorly defined irregular structures of variable and smaller average size (Fig. 7b).

In keeping with the findings of Pianet and co-workers for the self-association of synthetic procyanidins,[29] solutions of $[Pt^{II}(phen)(L^1\text{-}S,O)]^+$ in water also show a time dependent colloid formation process, resulting in micron-sized structures from solutions of high $[Pt^{II}(phen)(L^1\text{-}S,O)]^+$ concentration after aging (>7 days) as observed in TEM images shown in Fig. S6.‡ Preliminary Tyndall light-scattering experiments also confirm such an aging effect for concentrated solutions. Furthermore Atomic Force Microscopy (AFM) images of a spin-dried droplet of $[Pt^{II}(phen)(L^1\text{-}S,O)]Cl$ dissolved in acetonitrile reveal the presence of micron-sized "spaghetti-like" structures, remarkably similar in overall appearance and morphology to those obtained from TEM images (Fig. S7‡).

The possibility of a secondary helical structure was considered since the TEM images of the observed aggregates have a distinct size and shape. High-resolution TEM of samples prepared on a carbon-coated grid immediately after dilution of a solution containing nano-aggregates at concentrations above the CAC shows that the secondary structure appears to form from the agglomeration of 'strands' of $\{[Pt^{II}(phen)(L^1\text{-}S,O)]^+\}_nCl^-_y$ aligned parallel to each other, with a diameter of *ca.* 2 nm (Fig. 7c and S8‡). TEM images obtained from samples in diluted solutions left to 'age' (±2 h) do not show any structures in the nano-range as can be obtained from more concentrated freshly prepared samples. Evidently upon

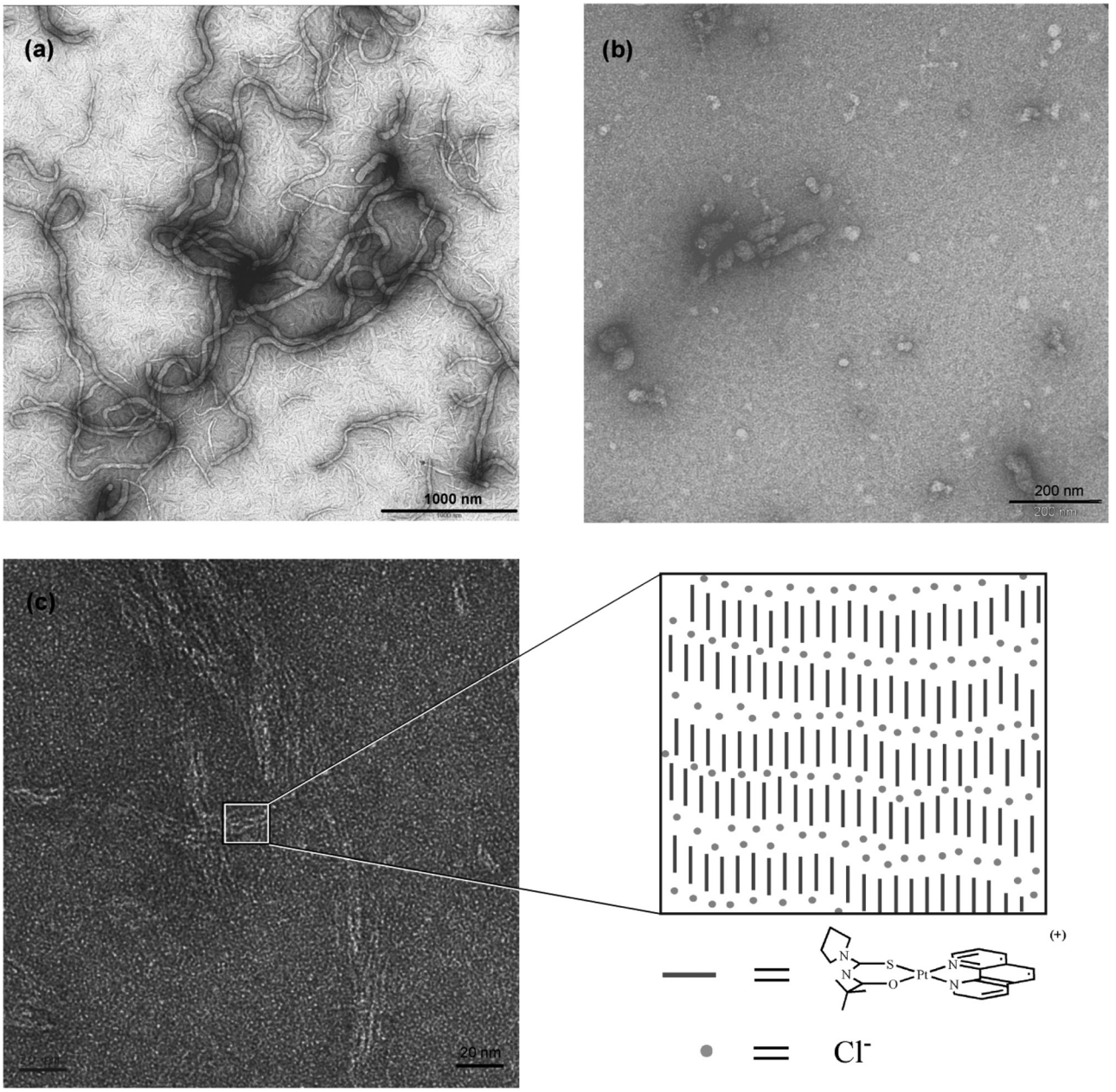


**Fig. 7** TEM images of [Pt$^{II}$(phen)(L$^1$-*S*,*O*)]Cl in (a) water (b) acetonitrile* and (c) freshly diluted water with uranyl acetate as a stain. *Staining in acetonitrile was done with uranyl acetate in ethanol.

dilution a type of dis-aggregation into presumably monomer and dimer species of [Pt$^{II}$(phen)(L$^1$-*S*,*O*)]Cl appears to take place.

On the basis of all the experimental data, it is tempting to postulate a qualitative aggregate growth model for the non-covalent association of [Pt$^{II}$(phen)(L$^1$-*S*,*O*)]$^+$ in water or water-rich solutions. Our data are consistent with a *region-specific* aggregation process of the hydrophobic planar [Pt$^{II}$(phen)(L$^1$-*S*,*O*)]$^+$ cations postulated in Scheme 1, strongly indicating a preferred cation–π "stacking" orientation, as found here and as suggested in previous studies with a related compound.[9,13] The driving force for the self-association or "stacking" of [Pt$^{II}$(phen)(L$^1$-*S*,*O*)]$^+$ is most likely to be the result of a combination of cation–π interactions accentuated by hydrophobic effects. Despite numerous efforts we have unfortunately not been able to obtain suitable single crystals for X-ray diffraction analysis.

An estimation of the approximate dimensions of the planar [Pt$^{II}$(phen)(L$^1$-*S*,*O*)]$^+$ cation from the data obtained from crystal structures of the related [Pt$^{II}$(en)(phen)]Cl$_2$ [34] and *cis*-[Pt$^{II}$(L$^1$-*S*,*O*)$_2$][35] complexes yields *ca.* 1.5 ± 0.2 nm, suggesting that a single 'strand' of [Pt$^{II}$(phen)(L$^1$-*S*,*O*)]$^+$ in a parallel co-planar stacking arrangement does not completely account for the *ca.* 20 nm nano-sized "spaghetti-like" structures observed in the

 

TEM images. We thus postulate that the nano-aggregates form by means of agglomeration of single strands of presumably individually stacked $[Pt^{II}(phen)(L^1\text{-}S,O)]^+$ cations in an offset cation–π arrangement, most probably stabilized by negatively charged chloride counter ions which may coil into the tube-like super-structures observed in Fig. 7c and S8.‡ The aggregation of the individual strands of co-planar cation–π stacked complexes may be facilitated by the chloride counter ion layers around the strands to form a positively charged "core" and a negatively charged outer layer of chloride ions to which the next positively charged strand may align due to electrostatic attractions. The overall diameter of the observed tube-like structures in TEM images is limited to ±20 nm in diameter. The apparent preferred accumulation of the cationic uranyl stain on the outer surface of the nano-structures in the TEM images is consistent with the aggregate formation model postulated here, in which the uranyl cations ion-pair with a negatively charged chloride 'layer' on the surface of the stacked cations $[Pt^{II}(phen)(L^1\text{-}S,O)]^+$ *via* π–cation interactions.

## Conclusions

$[Pt^{II}(phen)(L^1\text{-}S,O)]^+$ cations ($M^+$) 'self-associate' by non-covalent intermolecular cation–π interactions in acetonitrile solutions and water–acetonitrile mixtures of up to 30% (v/v) $D_2O$–$CD_3CN$ to form essentially dimer aggregates according to the $2M^+ \rightleftharpoons \{M^+\}_2$ model. This process is strongly favored in more polar water-rich solutions ($\Delta_r G^0_{CD3CN} = -7.0$ kJ mol$^{-1}$; $\Delta_r G^0_{30\%D2O-CD3CN} = -10.4$ kJ mol$^{-1}$), with the corresponding $K_D$ increasing from 17 ± 2 to 72 ± 8 M$^{-1}$ at 299.3 K from acetonitrile to 30% $D_2O$–$CD_3CN$ mixtures. The experimental data obtained suggest that the primary driving force for such phenomena is consistent with mainly cation–π stacking interactions, with the increase in the $K_D$ attributed to a favorable contribution to a negative $\Delta_r S^0$ as a result of the "hydrophobicity" of the quasi-aromatic nature of these complex cations. Increasing the water content from >30% to 100% (v/v) $D_2O$–$CD_3CN$ results in the extent of aggregation significantly increasing as a function of the $[Pt^{II}(phen)(L^1\text{-}S,O)]Cl$ concentration, culminating in the formation of nano-sized structures ("metallogels") consisting of up to *ca.* 735 mononuclear cations as determined by diffusion coefficients obtained by means of DOSY NMR spectroscopy, above a critical aggregation concentration (9.6–10.3 mM at 299.3 K). Experimental data suggest that in water, excessive positive electrostatic charge build-up in such structures may be partially offset by extensive cation–π interactions as well as by ion-pairing with $Cl^-$ anions. Uranyl acetate stained TEM images form freshly prepared samples of $[Pt^{II}(phen)(L^1\text{-}S,O)]Cl$ and the related $[Pt^{II}$(diimine)-(*N*,*N*-di(*n*-butyl)-*N*′-benzoylthiourea)]Cl compounds[14] provide convincing visual confirmation of the formation of extensive tube-like structures, *ca.* 20 nm in diameter. Such interesting behavior of $[Pt^{II}(phen)(L^1\text{-}S,O)]Cl$ in aqueous solution may have important implications for the demonstrated bioactivity[6,7] of these compounds.

## Experimental section

### Computational methods

Using the average observed chemical shift, $\delta_{obs}$, eqn (2) (where $\delta_i$ = $^1$H chemical shift, $\delta_i$, and $\alpha_i$ = mole fraction of species *i*) and the total concentration of reagents, we calculated for the reactions defined in the text the equilibrium constant(s), $K_i$, and chemical shifts, $\delta_i$, of individual species (monomers, dimer aggregates, trimer aggregates, ion-pairs, *etc.*).

$$\delta_{obs} = \sum_{i=n} \alpha_i \delta_i \quad (2)$$

This particular type of non-linear least squares optimisation calculation can be solved in several ways.[36] We opted to use a program called DIMER-$K_D$, written by us several years ago to fit data with a dimerization model[9] (the program utilizes the algorithm by Horman and co-workers[10]). When dealing with multiple equilibria we used the program called Dynafit version 3.[37] However, Dynafit version 3 uses the concentration of the species, $c_i$, and not mole fraction in the mass balance equations and signal response calculations. This problem was circumvented by multiplying eqn (2) with the total concentration, $C_T$, of the reagent of interest and after grouping terms, eqn (3) is obtained.

$$C_T \delta_{obs} = \sum_{i=n} c_i \delta_i \quad (3)$$

### Analytical instrumentation

$^1$H NMR and DOSY experiments were recorded in 5 mm tubes using a Varian Unity Inova 400 MHz spectrometer operating at 399.95 MHz or a Varian Unity Inova 600 MHz spectrometer equipped with an inverse-detection pulsed field gradient (idpfg) probe operating at 599.99 MHz. $^1$H NMR chemical shift referencing was done using the corresponding solvent peak with the HDO signal showing no chemical shift changes as a function of complex concentration. Diffusion coefficients were calculated using the Varian vnmrj software (version 2.1b) with a line broadening of 1.0 Hz. Experimental parameters: pulse sequence: Dbppste_cc (Bipolar Pulse Pair Stimulated Echo with Convection Compensation), $^1$H spectral width: 11 ppm, number of acquisitions varied from sample, recycling delay: 2 s, diffusion delay 50 ms, gradient-pulse duration 3.5 or 4.0 ms, 25 different values of *G*, the gradient magnitude, varying between 0.0107 and 0.449 Gm$^{-1}$ calibrated using the diffusion coefficient of HDO in $D_2O$.[38] Transmission electron microscopy imaging was done on a Zeiss 912 OMEGA EFTEM with a resolution of 0.35 nm and high resolution images were recorded with a High Resolution FEI/Tecnai F20 Cryo TWIN FEGTEM.

### Synthesis of complexes

All reagents and solvents were commercially available, and were used without further purification. The general method described by Morgan and Burstall for the synthesis of $Pt^{II}$(1,10-phenanthroline)$Cl_2$ was used from commercially available

$K_2[PtCl_4]$ and 1,10-phenanthroline monohydrate.[39] *N*-Pyrrolidyl-*N*-(2,2-dimethylpropanoyl)thiourea was prepared as described in the literature.[35] [*N*-pyrrolidyl-*N*-(2,2-dimethylpropanoyl)-thioureato](1,10-phenanthroline) platinum(II) chloride was prepared as previously described.[13]

### Characterization

Previously the NMR characterization of $[Pt^{II}(phen)(L^1\text{-}S,O)]Cl$ was done in acetonitrile-$d_3$ by $^1H$, $^1H$-COSY, $^1H^{15}N$-HMBC NMR experiments.[13] $^1H$ NMR assignments to the various protons of $[Pt^{II}(phen)(L^1\text{-}S,O)]Cl$ could be made from the $^1H$-COSY spectra, although one unambiguous assignment for the $H^{2/9}$ protons was outstanding. Previously the diimine proton of the 1,10-phenanthroline ligand *trans* to the sulphur atom of the coordinated *N*-pyrrolidyl-*N*-(2,2-dimethylpropanoyl)thiourea was assigned based on the expectation of more de-shielded as a result of a more pronounced *trans* effect induced by the sulphur donor atom.[9] The 1-D NOE spectra (Fig. S9‡) showed a positive NOE for the most de-shielded proton of the 1,10-phenanthroline ligand upon excitation of the methyl protons of the *N*-acyl-*N*,*N*-dialkylthiourea ligand (Fig. S9a‡) and *vice versa* (Fig. S9b‡). Moreover, upon selective irradiation of the methyl protons $H^{1'}$, NOE's were observed for $H^2$ and $H^{a'}$ which now allows for the unambiguous assignment of all $^1H$ NMR resonances of the *N*-pyrrolidyl group ($H^{a',b'}$ and $H^{a,b}$), previously tentatively assigned on the basis of the relative magnitude of the relevant $^{195}Pt$-$^{13}C$ coupling constants.[35] Hence the unambiguous assignment of the most de-shielded 1,10-phenanthroline proton and methylene protons of the *N*-acyl-*N*,*N*-dialkylthiourea group could be assigned as $H^2$ and $H^{a'}$ respectively, Fig. 1.

## Acknowledgements

We acknowledge the support of Dr Jacobus Brand for his assistance in NMR and particularly the DOSY spectroscopy. Financial support from Stellenbosch University, the National Research Foundation (bursary to I. Kotzé,) as well as Anglo-platinum Ltd is gratefully acknowledged.

## Notes and references

1 J. A. A. W. Elemans, A. E. Rowan and R. J. M. Nolte, *J. Am. Chem. Soc.*, 2002, **124**, 1532–1540.
2 W. Lu, D. A. Vicic and J. K. Barton, *Inorg. Chem.*, 2005, **44**, 7970–7980.
3 A. M. Krause-Heuer, N. J. Wheate, M. J. Tilby, D. G. Pearson, C. J. Ottley and J. R. Aldrich-Wright, *Inorg. Chem.*, 2008, **47**, 6880–6888.
4 F. H. Stootman, D. M. Fisher, A. Rodgerc and J. R. Aldrich-Wright, *Analyst*, 2006, **131**, 1145–1151.
5 S. Rafique, M. Idrees, A. Nasim, H. Akbar and A. Amin, *Biotechnol. Mol. Biol. Rev.*, 2010, **5**, 38–45.
6 T. J. Egan, K. R. Koch, P. L. Swan, C. Clarkson, D. A. Van Schalkwyk and P. J. Smith, *J. Med. Chem.*, 2004, **47**, 2926–2934.
7 Y.-S. Wu, K. R. Koch, V. R. Abratt and H. H. Klump, *Arch. Biochem. Biophys.*, 2005, **440**, 28–37.
8 H. H. Klump, K. R. Koch and C. T. S. Lin, *Afr. J. Chem.*, 2006, **102**, 264–266.
9 K. R. Koch, C. Sacht and C. Lawrence, *J. Chem. Soc., Dalton Trans.*, 1998, 689–695.
10 I. Horman and B. Dreux, *Helv. Chim. Acta*, 1984, **67**, 754–764.
11 L. Fielding, *Tetrahedron*, 2000, **56**, 6151–6170.
12 A. Macchioni, A. Romani, C. Zuccaccia, G. Guglielmetti and C. Querci, *Organometallics*, 2003, **22**, 1526–1533.
13 I. A. Kotzé, W. J. Gerber, J. M. Mckenzie and K. R. Koch, *Eur. J. Inorg. Chem.*, 2009, **12**, 1626–1633.
14 Y.-S. Wu, *PhD dissertation*, University of Cape Town, 2002.
15 P. S. Pregosin, *Prog. Nucl. Magn. Reson. Spectrosc.*, 2006, **19**, 261–288.
16 F. Song, S. J. Lancaster, R. D. Cannon, M. Schormann, S. M. Humphrey, C. Zuccaccia, A. Macchioni and M. Bochmann, *Organometallics*, 2005, **24**, 1315–1328.
17 T. J. Egan, *Trends Parasitol.*, 2006, **22**, 235–237.
18 I. Z. Steinberg and A. H. Scheraga, *J. Biol. Chem.*, 1963, **238**, 172–181.
19 P. Doty and G. E. Myers, *Discuss. Faraday Soc.*, 1953, **13**, 51–58.
20 W. Kauzmann;, C. B. Anfinsen, M. L. Anson, K. Bailey and J. T. Edsall, *Adv. Protein Chem.*, 1959, **14**, 1–63.
21 H. A. Scheraga, *J. Phys. Chem.*, 1961, **66**, 1071–1072.
22 C. H. Wohlfarth, *Landolt-Börnstein – Group IV Physical Chemistry*, Springer, Berlin Heidelberg, 2008, vol. 17, pp. 117–121.
23 H.-J. Schneider, *Angew. Chem., Int. Ed. Engl.*, 1991, **30**, 1417–1436.
24 C. A. Hunter and J. K. M. Sanders, *J. Am. Chem. Soc.*, 1990, **112**, 5525–5534.
25 T. D. W. Claridge, *High-Resolution NMR Techniques in Organic Chemistry – Tetrahedron Organic Chemistry Series*, Pergamon, Oxford, 1999, 19.
26 H. Friebolin, *Basic One- and Two-Dimensional NMR Spectroscopy*, Wiley-VCH, Wheinheim, 2005.
27 P. J. Hore, *Nuclear Magnetic Resonance*, Oxford, 1995.
28 V. I. Bakhmutov, *Practical NMR Relaxation for Chemists*, John Wiley and Sons Ltd., London, 2004.
29 I. Pianet, Y. André, M. A. Ducasse, I. Tarascou, J. C. Lartigue, N. Pinaud, E. Fouquet, E. J. Dufourc and M. Laguerre, *Langmuir*, 2008, **24**, 11027–11035.
30 L. Luchetti and G. Mancini, *Langmuir*, 2000, **16**, 161–165.
31 H. J. Hwang, S. K. Lee, S. Lee and J. W. Park, *J. Chem. Soc., Perkin Trans. 2*, 1999, 1081–1086.
32 G. Bellachioma, G. Ciancaleoni, C. Zuccaccia, D. Zuccaccia and A. Macchioni, *Coord. Chem. Rev.*, 2008, **252**, 2224–2238.
33 H.-L. Zhang, G.-H. Chen and S.-J. Han, *J. Chem. Eng. Data*, 1997, **42**, 526–530.

 

34 M. Kato and J. Takahashi, *Acta Crystallogr., Sect. C: Cryst. Struct. Commun.*, 1999, **55**, 1809–1812.
35 A. N. Mautjana, J. D. S. Miller, A. Gie, S. A. Bourne and K. R. Koch, *Dalton Trans.*, 2003, 1952–1960.
36 M. Meloun, J. Havel and E. Högfeldt, *Computation of Solution Equilibria – A Guide to Methods in Potentiometry, Extraction, and Spectrophotometry*, Ellis Horwood, Chichester, 1987.
37 P. Kuzmic, *Anal. Biochem.*, 1996, **237**, 260–273.
38 B. Antalek, *Concepts Magn. Reson.*, 2002, **14**, 225–258.
39 G. T. Morgan and F. H. Burstall, *J. Chem. Soc.*, 1934, 965–971.